

## Seismic Vulnerability Analysis of Single-Story Reinforced Concrete Industrial Buildings with Seismic Fortification

Jieping Liu<sup>1</sup>, Lingxin Zhang<sup>1,\*</sup>, Haohao Zhang<sup>2</sup> and Tao Liu<sup>1</sup>

**Abstract:** As there is a lack of earthquake damage data for factory buildings with seismic fortifications in China, seismic vulnerability analysis was performed by numerical simulation in this paper. The earthquake-structure analysis model was developed with considering the influence of uncertainties of the ground motion and structural model parameters. The small-size sampling was conducted based on the Latin hypercube sampling and orthogonal design methods. Using nonlinear analysis, the seismic vulnerability curves and damage probability matrix with various seismic fortification intensities (SFI) were obtained. The seismic capacity of the factory building was then evaluated. The results showed that, with different designs at different SFIs, the factory building could consistently achieve the three seismic fortification objectives. For the studied factory buildings with the SFI of 6, they satisfied the seismic fortification requirements of “no damage in moderate earthquakes, mendable in strong earthquakes”; for those buildings with SFIs of 7 and 8, the requirement of “no collapsing in super strong earthquakes” was generally met; while for those with SFIs of 9, the requirement of “mendable in moderate earthquakes” was almost satisfied. The results showed factory buildings designed with low SFIs are better at achieving the seismic fortification objectives than those designed with high SFIs.

**Keywords:** Seismic vulnerability analysis, uncertainty, latin hypercube sampling, orthogonal design, nonlinear time history analysis, factory buildings.

### 1 Introduction

With the rapid development of industrialization in China, there are a growing number of industrial enterprises that support the development of the national economy. Most of those enterprises are located in an earthquake zone that is above the seismic fortification intensity (SFI) of 7. Industrial buildings have different characteristics than other civil constructions. Industrial enterprises can be seen as a system in which these industrial buildings are the core structural component. Once industrial buildings are heavily damaged or collapsed, there would be direct or indirect economic losses caused by the damage of the building structures, indoor property (equipment, finished or semi-finished products, etc.), and the

---

<sup>1</sup> Key Laboratory of Earthquake Engineering and Engineering Vibration, Institute of Engineering Mechanics, China Earthquake Administration, Nangang District, Harbin, 150080, China.

<sup>2</sup> School of Civil Engineering, Southeast University, Xuanwu District, Nanjing, 211189, China.

\* Corresponding Author: Lingxin Zhang. Email: lingxin\_zh@126.com.

shutdown or reduction of production. Therefore, the earthquake damage of industrial buildings can have a great impact on the national economy. For instance, in the 1976 Tangshan 7.8 Earthquake, the industrial factories in Tangshan and Tianjin were caused to shut down completely or partially, and the severe economic loss was estimated to be 10 billion yuan. In the 2008 Wenchuan 8.0 Earthquake, the huge disaster affected Sichuan, Gansu, Shanxi province as well as other disaster areas, and there was significant damage to the industrial raw material providers, manufacturing, light industry, electronic information industry, national defense industry, and many other industries [*Earthquake relief in Wenchuan Great Earthquake* (Book 4: Earthquake disaster)].

At present, single-story reinforced concrete (RC) column buildings are employed in a large proportion of the existing industrial structures in China. To efficiently mitigate earthquake disasters, it is critical to for these single-story RC column factory buildings to have a good seismic resistance capacity. The seismic vulnerability analysis of building structures provides a method for earthquake disaster loss assessment, and it is the basis for seismic damage prediction. The comprehensive seismic capacity level of structures is given by the seismic vulnerability analysis, and the weak parts of structures can be identified to improve seismic design methods and structure designs to reduce the earthquake related losses.

The vulnerability analysis method for industrial factory buildings is mainly based on the earthquake disaster data statistics and numerical analysis. For the RC column factory buildings without seismic fortification, the seismic vulnerability analysis can be carried out based on the seismic data of the Haicheng Earthquake and Tangshan Earthquake. As for the RC column factory buildings with seismic fortification, there is a lack of necessary seismic data, and that limits the use of statistical analysis due to the small number of samples.

Regarding the seismic vulnerability analysis of the current numerical factory building, current research has focused more on the uncertainties of ground motion parameters and less on the uncertainties of structural parameters [Hamed, Nuno, Paulo et al. (2016); Fuchs, Keiler and Glade (2017); Mirko, Peter and Matjaž (2014)]. In this study, by using a numerical simulation method, the seismic vulnerability curves of single-story RC factory buildings with seismic fortification are determined. The influences of the uncertainties of ground motion parameters and structure parameters on the seismic vulnerability analysis are fully considered. The small-size sampling is performed by the Latin hypercube sampling method and the orthogonal design method. Then, the earthquake-structure finite element analysis (FEA) models are built. SAP2000 software is used for the nonlinear time history analysis. Finally, the seismic vulnerability curves and damage probability matrix of RC factory buildings with various SFIs are determined, and the seismic capacity of the factory buildings is evaluated. This study improves the understanding of the seismic vulnerability and seismic performance of single-story RC industrial buildings.

## **2 Selection of sampling methods**

In many numerical methods of vulnerability analysis, the Monte Carlo (MC) method and methods based on the reduction of variance technology are commonly used. However, in practical engineering, large-size sample tests are prohibitively expensive or difficult to obtain, so small-size sampling techniques are commonly employed. The common small-size sampling methods typically used are the Latin hypercube sampling technique [Mirko,

Peter and Matjaž (2014); Felipe, Gerhard and Vladimir (2010); Wu, Wang, Patrick et al. (2017); Ricardo (2016)], the Quasi-Monte Carlo method [Roy, Roy and Vasu (2013); Lam, Hu and Yang (2017)], the orthogonal design [Seymour and Ahsan (2014); Chen, Liu, Li et al. (2017); Matjaz (2009)], and the uniform design [Zhang, Alberdi and Khandelwal (2016); Lee, Manić, Bulajić et al. (2015); Mauro, Gustavo and Saúl (2018)].

Of the mentioned methods, the Latin hypercube sampling technique has the advantages of fast convergence speed, small sample size, strong versatility, and ease of use for practical engineering. In the model-based standard toolbox of Matlab, the Latin hypercube sampling and hierarchical Latin hypercube sampling technology are embedded. This toolbox provides a program for sampling and parameter matching and also a model evaluation program to evaluate the Latin hypercube sampling method. The advantages of the orthogonal design method are that it provides a uniform dispersion, tidiness, and good comparative evaluation. The orthogonal design method also has a property of “equality”, which means that the level of each factor is treated equally without discrimination, and all the horizontal combinations of any two factors are treated equally without discrimination. Therefore, to reduce the number of samples and improve the computation efficiency, the Latin hypercube sampling technique was chosen and combined with the orthogonal design for the selection of sample in the vulnerability analysis.

### **3 Representative factory building**

The seismic vulnerability of single-story RC factory buildings with seismic fortification was analyzed by using the sampling technique presented in Section II to first establish the representative structure. For this purpose, the codes for seismic design of buildings (GBJ-89), (GB50011-2001), (GB50011-2001, 2008 Edition) and (GB50011-2010) were compared in terms of the design contents of the single-story RC Column factory building, its structural layout and member selection, seismic calculations, and details of seismic design. There are no significantly large changes between the different versions listed above.

There are a few small differences between the current code (GB50011-2010) and the previous code (GB50011-2001) regarding the structure layout, seismic calculations, and structural details of single-story factory buildings with RC columns. The content of (GB50011-2001) has some modifications and supplementations to the (GBJ-89) code. Therefore, this paper used the (GB50011-2010) for the designing of models of typical single-story RC column factory buildings with different seismic fortifications.

#### **3.1 Design of representative factory building**

A factory building in Dujiangyan of Sichuan province was taken as the prototype single-story single-span RC column frame building. This design had a light roof, a span of 18 m, width of 6 m, longitudinal length of 90 m, lower portion height of columns of 8.1 m, upper portion height of columns of 3.9 m, and two sets of 20/5t heavy duty cranes were placed with site-class II specifications. The concrete was C30, and the steel was HPB235. The space and plane models of the factory building are shown in Fig. 1 and Fig. 2.

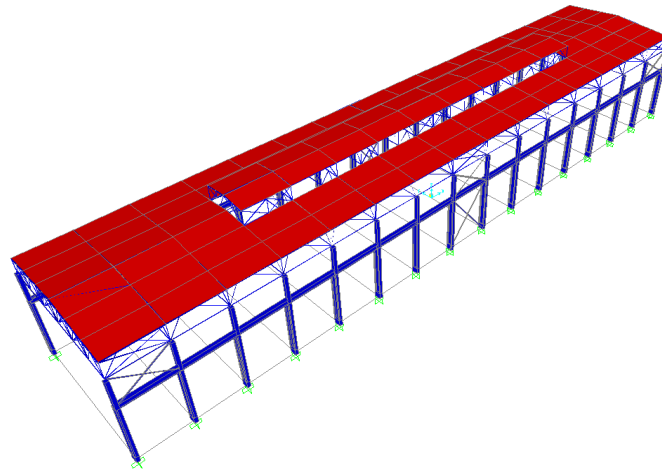


**Figure 1:** Spatial integral model of factory building

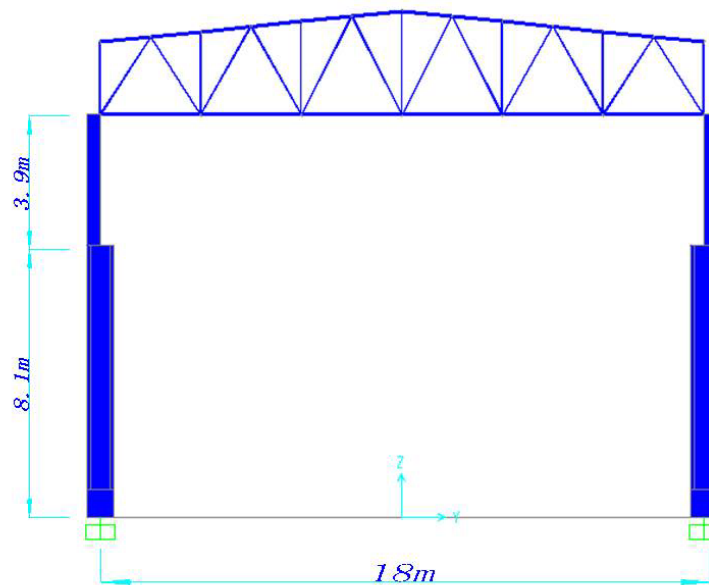


**Figure 2:** Plane model of factory building

Using the code (GB50011-2010), the model factory building is designed to be a representative single-story RC column factory building with seismic design with seismic fortification intensities of 6, 7, 8, and 9. The parameters of the columns for the model are shown in Tab. 1.

**Table 1:** Design parameters of bent column

Intensity	Portion of column	Shape of cross section	Size of cross section* (mm <sup>2</sup> )	Reinforcement**
6	Upper	Rectangle	400×400	2Φ18
	Lower	I-type	800×400×100×100	2Φ16 and 2Φ20
7	Upper	Rectangle	400×400	2Φ20
	Lower	I-type	800×400×100×100	2Φ16 and 2Φ25
8	Upper	Rectangle	400×500	4Φ20
	Lower	I-type	1000×400×100×200	4Φ20 and 2Φ25
9	Upper	Rectangle	400×500	4Φ25
	Lower	I-type	1000×400×100×200	6Φ25

Notes: \*Cross section size of column=cross section height of column×width of flange×web thickness×flange thickness; \*\* a single side reinforcement is given, but this reinforcement is placed on both sides in the model.

### 3.2 Seismic response analysis method for single-story RC column factory building

By using the analysis software SAP2000, the nonlinear seismic response of each sample of the structural seismic model system were analyzed, which based on the nonlinear seismic response analysis method of the single-story RC column factory buildings in Li [Li (2010)]. In this method, finite element models of spatial multi-particle beam and column-bar element were adopted. The Takeda trilinear model was chosen for the nonlinear analysis and is shown in Fig. 3. In this figure P1 and D1 are the first yield strength and deformation of component, P2 and D2 are the second yield strength and deformation of component respectively.

The nonlinearity of columns, beams, and braces are mainly reflected in the properties of the plastic hinge. Every plastic hinge was simulated by discrete hinge points, all plastic deformation occurred in the hinge points, and the corresponding length was defined. The plastic hinge had the axial force hinge and the PMM hinge (axial force bending moment coupling hinge), and this plastic hinge model is shown in Fig. 4. For computation efficiency and model the nonlinear response, consideration of the seismic damage materials of factory buildings was made by adding a few plastic hinges in positions corresponding with high damage probability. These added plastic hinges included PMM hinges set in the upper and lower columns, as well as axial force hinges set in supports between the upper columns, between the lower columns, and in vertical supports between the roof trusses. The details of the proposed method, as well its reliability and effectiveness, have been verified previously [Li (2010)].

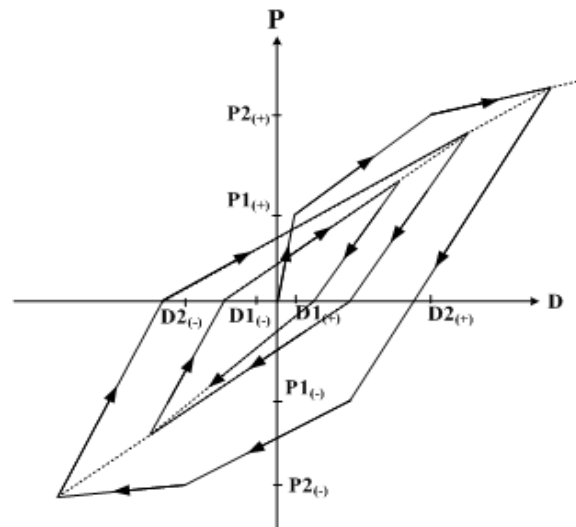


**Figure 3:** Takeda trilinear model

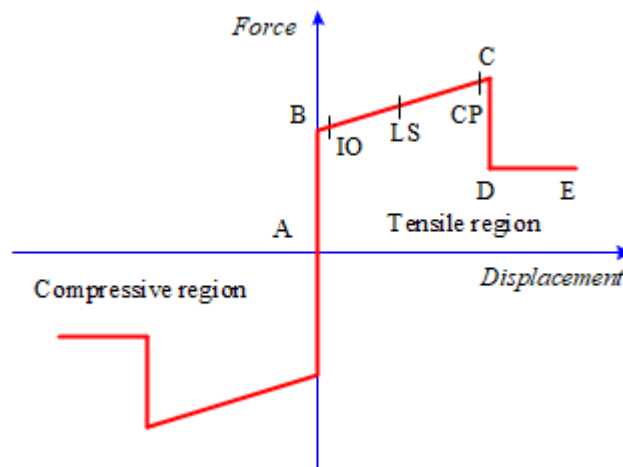


**Figure 4:** Plastic hinge model in SAP2000

#### 4 Parameter selection and statistical sampling in seismic vulnerability analysis

Structural seismic vulnerability analysis is based on probability analysis. There are four main aspects that affect vulnerability analysis. These aspects are structural parameters, seismic hazard analysis, numerical simulation analysis method, and the model establishment and vulnerability derivation. Of these four aspects, the vulnerability analysis is affected by the limit state partition method and the analysis method, and the uncertainty of its parameters cannot be evaluated by objective criteria. Therefore, in this paper, the uncertainty of parameters in the limit state partition method and the analysis method were not considered. Nevertheless, the uncertainties of ground motion parameters and structural model parameters were considered.

**4.1 Uncertainty of structural model parameters**

The parameters of the structural model include section size, mass, material parameters, hysteresis model, and damping. The component section size and structure model mass can usually be accurately measured, so they are considered as the certain parameters.

The initial stiffness of the hysteresis model in the nonlinear analysis is directly affected by material parameters of the components. The material parameters are the rebar yield strength  $f_y$ , steel elastic modulus  $E_s$ , concrete ultimate compressive strength  $f_c$ , and concrete elastic modulus  $E$ . These four parameters are selected as the uncertainty parameters in this paper.

The above four material parameters are sampled according to the Latin hypercube sampling technique. As these parameters follow the lognormal distribution, only three variable values are needed to represent the material parameters. These key values are the mean value, mean value plus a standard deviation, and mean value minus a standard deviation. The statistical parameters of these four uncertainty parameters are given in the literature [Lü, Yu, Pan et al. (2010)]. The sampling values used in this paper are based on the literature and are listed in Tab. 2.

From previous studies [Howard, Hwang and Jaw (1990)], five parameters are needed in the Takeda trilinear model and only three uncertain parameters are needed. These parameters are the yield stiffness reduction coefficient  $\alpha_1$ , yield shear strain  $\gamma_y$ , viscous damping ratio  $\zeta$ . The representative values used of these uncertain parameters were obtained from tests and shown to be reasonable, and are listed in Tab. 2.

**Table 2:** Ground motion and structure uncertainty parameters and their representative values

No.	Uncertainty parameters	Representative Values		
1	$a/v$ ( $g/ms^{-1}$ )	$a/v \leq 0.8$	$0.8 < a/v < 1.2$	$a/v \geq 1.2$
2	$f_y \times 10^5$ ( $kN/m^2$ )	2.35	2.54	2.16
3	$f_c \times 10^3$ ( $kN/m^2$ )	16.7	18.27	15.13
4	$E_s \times 10^8$ ( $kN/m^2$ )	2.0	2.12	1.88
5	$E \times 10^7$ ( $kN/m^2$ )	3.0	3.3	2.7
6	$\alpha_1$	0.17	0.25	0.1
7	$\gamma_y$	0.0025	0.003	0.002
8	$\zeta$	0.05	0.06	0.02

**4.2 Uncertainty of parameters of ground motion**

The natural ground motion records were selected as earthquake inputs. In the seismic vulnerability analysis, the influence of earthquake magnitude, epicenter distance, and site conditions should be considered. These three variables are regarded as the selection criteria to define different types of ground motion. The ground motion records were divided into three types of ground motion while considering the influence of uncertainties.

There are many parameters representing seismic uncertainty. These parameters can reflect both the ground motion and the characteristics of the response spectrum. Note that  $a$  and  $v$  are the peak of horizontal seismic acceleration and velocity and have been widely used in previous studies as the  $a/v$  ratio. This  $a/v$  ratio can show the characteristics of seismic structural parameters, site conditions and spectral parameters of the ground motion record [Zhu, Heidebrecht and Tso (1988)]. Other investigations [Banon, Biggs and Irvine (1981)] have concluded that a low  $a/v$  ratio means that the main frequency of the ground motion is low, the response spectrum is wide, the period of motion is long, the magnitude is medium to large, the epicentral distance is long, and the site soil period is long. Conversely, a high  $a/v$  ratio means that the main frequency of ground motion is high, the response spectrum is narrow, the period of motion is short, the magnitude is from small to medium, the epicentral distance is short, and the site soil period is short. Therefore, the  $a/v$  ratio is used in this paper to fully consider the effects of earthquake magnitude, epicentral distance, and site conditions on the structural seismic vulnerability.

Natural ground motion is classified three types [Zhu, Heidebrecht and Tso (1988)]: when  $a/v < 0.8 \text{ g/ms}^{-1}$ ; when  $0.8 \text{ g/ms}^{-1} \leq a/v \leq 1.2 \text{ g/ms}^{-1}$ ; and when  $a/v > 1.2 \text{ g/ms}^{-1}$ . Using this classification, 45 ground motion records in the database of Pacific Earthquake Engineering Research Center (PEER) were selected and classified and are shown in Tab. 3. This table ranks the ground motions by an ascending  $a/v$  value. Using the classification scheme, the first class includes the ground motions with numbers 1-15, the second class includes the ground motions with numbers 16-30, and the third class includes the ground motions with numbers 31-45.

**Table 3:** 45 ground motion records

No.	a_max	v_max	a/v	Magnitude	Epicentral Distance	Site Class	Name and Location of Earthquakes
1	0.348	159.0	0.22	7.6	0.24	C	Chi-Chi,Taiwan
2	0.016	5.5	0.29	7.1	49.9	B	Duzce,Turky
3	0.008	2.7	0.30	7.1	135.7	B	Duzce,Turky
4	0.016	4.4	0.36	7.1	101.7	C	Duzce,Turky
5	0.008	2.2	0.36	7.6	154.59	C	Chi-Chi,Taiwan
6	0.090	18.5	0.49	7.6	100.53	D	Chi-Chi,Taiwan
7	0.099	20.0	0.50	7.6	50.89	D	Chi-Chi,Taiwan
8	0.007	1.4	0.50	6.8	203.00	B	Borrego Mtn
9	0.038	7.4	0.51	7.1	193.30	D	Duzce,Turky
10	0.266	46.8	0.57	6.5	9.30	D	Imperial Vally
11	0.348	60.0	0.58	7.1	8.20	C	Duzce,Turky
12	0.057	8.3	0.69	6.2	64.40	C	Morgan Hill
13	0.218	31.4	0.69	6.0	10.10	B	N.Palm Springs
14	0.154	20.2	0.76	7.1	44.60	B	Cape Mendocino
15	0.111	14.2	0.78	7.1	0.90	B	Duzce,Turky
16	0.594	73.3	0.81	6.0	8.20	B	N.Palm Springs

17	0.154	18.9	0.81	5.8	17.60	C	Livemore
18	0.051	5.9	0.86	6.7	80.00	A	Northridge
19	0.434	49.2	0.88	5.7	3.10	B	Coyote Lake
20	0.023	2.6	0.88	5.8	20.30	B	Livemore
21	0.653	72.9	0.90	7.6	7.31	C	Chi-Chi,Taiwan
22	0.277	30.3	0.91	7.6	15.28	A	Chi-Chi,Taiwan
23	0.212	21.8	0.97	6.0	9.80	C	Whittier Narrows
24	0.025	2.5	1.00	6.0	28.80	B	Whittier Narrows
25	0.053	5.3	1.00	6.0	45.70	C	N.Palm Springs
26	0.044	4.3	1.02	6.2	30.30	B	Morgan Hill
27	0.271	26.3	1.03	5.7	4.50	C	Coyote Lake
28	0.519	46.9	1.11	6.5	1.00	C	Imperial Vally
29	0.098	8.6	1.14	6.4	50.70	C	Coalinga
30	1.497	127.4	1.18	7.1	8.50	A	Cape Mendocino
31	0.046	3.6	1.28	6.7	47.30	A	Northridge
32	0.275	21.2	1.30	6.5	10.60	C	Imperial Vally
33	0.099	5.8	1.71	6.0	46.70	A	N.Palm Springs
34	0.121	6.9	1.75	6.0	73.20	C	N.Palm Springs
35	0.072	4.1	1.76	5.8	31.00	B	Livemore
36	0.039	2.2	1.77	5.7	31.20	C	Coyote Lake
37	0.048	2.7	1.78	6.2	71.20	C	Morgan Hill
38	0.348	17.4	2.00	6.2	12.80	C	Morgan Hill
39	0.059	2.7	2.19	6.7	101.30	B	Northridge
40	0.039	1.7	2.29	6.0	24.60	A	Whittier Narrows
41	0.069	2.90	2.38	6.2	16.20	A	Morgan Hill
42	0.065	2.30	2.83	6.0	46.30	B	Whittier Narrows
43	0.060	2.10	2.86	6.0	52.40	B	Whittier Narrows
44	0.103	3.40	3.03	5.7	9.30	A	Coyote Lake
45	0.229	7.10	3.23	7.1	33.80	B	Cape Mendocino

#### ***4.3 Establishment of structure-motion model***

According to Sections IV-A and IV-B, 7 structural uncertain parameters and 1 ground motion uncertain parameter were selected. The 3 representative values were selected for each parameter. Using those selections, the MBC toolbox in Matlab was used for the Latin hypercube sampling technique. As only three tests are needed in this sampling technique, the number of tests was reduced in comparison to other techniques. To increase the sample number, the orthogonal design was combined with the Latin hyper cubic sampling techniques, which are shown in Tab. 4 and Tab. 5. A total of 27 sets of structural seismic analysis samples were calculated. Each group of samples contains 15 different ground motion records, so a total of 405 structural-motion analysis samples were established.

**Table 4:** Design table of Latin hypercube sampling data

No.	1 a/v g/ms <sup>-1</sup>	2 f <sub>y</sub> ×10 <sup>5</sup> KN/m <sup>2</sup>	3 f <sub>c</sub> ×10 <sup>3</sup> KN/m <sup>2</sup>	4 E <sub>s</sub> ×10 <sup>8</sup> KN/m <sup>2</sup>	5 E×10 <sup>7</sup> KN/m <sup>2</sup>	6 α <sub>1</sub>	7 γ <sub>y</sub>	8 ζ
1	a/v ≤ 0.8	2.35	15.13	2.0	3.3	0.25	0.0025	0.05
2	0.8 < a/v < 1.2	2.54	18.27	2.12	3.0	0.1	0.002	0.02
3	a/v ≥ 1.2	2.16	16.7	1.88	2.7	0.17	0.003	0.06

**Table 5:** The Orthogonal design table

No.	1 a/v g/ms <sup>-1</sup>	2 f <sub>y</sub> ×10 <sup>5</sup> KN/m <sup>2</sup>	3 f <sub>c</sub> ×10 <sup>3</sup> KN/m <sup>2</sup>	4 E <sub>s</sub> ×10 <sup>8</sup> KN/m <sup>2</sup>	5 E×10 <sup>7</sup> KN/m <sup>2</sup>	6 α <sub>1</sub>	7 γ <sub>y</sub>	8 ζ
1	a/v ≤ 0.8	2.35	16.7	2.0	3.0	0.17	0.0025	0.05
2	a/v ≤ 0.8	2.35	16.7	2.0	3.3	0.25	0.003	0.06
3	a/v ≤ 0.8	2.35	16.7	2.0	2.7	0.1	0.002	0.02
4	a/v ≤ 0.8	2.54	18.27	2.12	3.0	0.17	0.0025	0.06
5	a/v ≤ 0.8	2.54	18.27	2.12	3.3	0.25	0.003	0.02
6	a/v ≤ 0.8	2.54	18.27	2.12	2.7	0.1	0.002	0.05
7	a/v ≤ 0.8	2.16	15.13	1.88	3.0	0.17	0.0025	0.02
8	a/v ≤ 0.8	2.16	15.13	1.88	3.3	0.25	0.003	0.05
9	a/v ≤ 0.8	2.16	15.13	1.88	2.7	0.1	0.002	0.06
10	0.8 < a/v < 1.2	2.35	18.27	1.88	3.0	0.25	0.002	0.05
11	0.8 < a/v < 1.2	2.35	18.27	1.88	3.3	0.1	0.0025	0.06
12	0.8 < a/v < 1.2	2.35	18.27	1.88	2.7	0.17	0.003	0.02
13	0.8 < a/v < 1.2	2.54	15.13	2.0	3.0	0.25	0.002	0.06
14	0.8 < a/v < 1.2	2.54	15.13	2.0	3.3	0.1	0.0025	0.02
15	0.8 < a/v < 1.2	2.54	15.13	2.0	2.7	0.17	0.003	0.05
16	0.8 < a/v < 1.2	2.16	16.7	2.12	3.0	0.25	0.002	0.02
17	0.8 < a/v < 1.2	2.16	16.7	2.12	3.3	0.1	0.0025	0.05
18	0.8 < a/v < 1.2	2.16	16.7	2.12	2.7	0.17	0.003	0.06
19	a/v ≥ 1.2	2.35	15.13	2.12	3.0	0.1	0.003	0.05
20	a/v ≥ 1.2	2.35	15.13	2.12	3.3	0.17	0.002	0.06
21	a/v ≥ 1.2	2.35	15.13	2.12	2.7	0.25	0.0025	0.02
22	a/v ≥ 1.2	2.54	16.7	1.88	3.0	0.1	0.003	0.06

23	$a/v \geq 1.2$	2.54	16.7	1.88	3.3	0.17	0.002	0.02
24	$a/v \geq 1.2$	2.54	16.7	1.88	2.7	0.25	0.0025	0.05
25	$a/v \geq 1.2$	2.16	18.27	2.0	3.0	0.1	0.003	0.02
26	$a/v \geq 1.2$	2.16	18.27	2.0	3.3	0.17	0.002	0.05
27	$a/v \geq 1.2$	2.16	18.27	2.0	2.7	0.25	0.0025	0.06

### 5 Vulnerability analysis based on nonlinear time history analysis

The sampling technique mentioned above was used to obtain the structure-motion analysis samples of the single-story RC column factory building with SFIs of 6, 7, 8, and 9 for the nonlinear seismic response analysis. Using these samples, the vulnerability analysis results were obtained through statistical analysis.

The failure state in the vulnerability analysis of structures is divided into 5 levels that are classified as no damage, minor damage, medium damage, severe damage, and collapse. The limit state is characterized based on the maximum inter-story displacement angle of the structure. The inter-story displacement angle limitation of each failure state of a single-story RC column building is based on a large set of experimental data concerning of earthquake disaster damage in the literature and shown in Tab. 6 [Li (2011)].

**Table 6:** Limit value of damage level of single-story factory buildings with RC columns

State of failure	No damage	Minor damage	Medium damage	Severe damage	Collapse
Inter-story displacement angle	$\theta < 0.25\%$	$0.25\% < \theta \leq 0.5\%$	$0.5\% < \theta \leq 0.83\%$	$0.83\% < \theta \leq 2.0\%$	$2.0\% < \theta$

If the strength of ground motion is indicated by the peak of ground motion acceleration (PGA) and the structural response is characterized by the maximum inter-story displacement angle  $\theta_{max}$ , then the structural vulnerability can be expressed as follows:

$$F(x) = P[\theta_D \geq \theta_C | PGA = x] \quad (1)$$

where the variable  $x$  is the strength level of the ground motion and is equal to the PGA;  $\theta_D$  is the maximum inter-story displacement angle at the strength level of  $x$ ;  $\theta_C$  is the lower limit of the maximum inter-story displacement angle at the strength level of  $x$ .

Assuming that both  $\theta_D$  and  $\theta_C$  obey the lognormal distribution, the probability of exceeding the limit state  $P_f$  of the structure experiencing the ground motion can be obtained by the following equation:

$$P_f(PGA = x) = \Phi \left( \frac{-\ln(\theta_C / \theta_D)}{\sqrt{\sigma_{\ln C}^2 + \sigma_{\ln D}^2}} \right) = \Phi \left( \frac{\ln(e^A(x)^B / \theta_C)}{\sqrt{\sigma_{\ln C}^2 + \sigma_{\ln D}^2}} \right) \quad (2)$$

where  $\sigma_{\ln C}$  and  $\sigma_{\ln D}$  are the logarithmic standard deviation of  $\theta_C$  and  $\theta_D$ . For a RC structure with PGA as the ground motion input,  $(\sigma_{\ln C}^2 + \sigma_{\ln D}^2)^{1/2}$  can be taken as 0.5 [Li (2011)].

Through Eq. (2), the probability of a structure surpassing a certain limit state under different strength levels of ground motions can be calculated. Then, the damage probability matrix and the corresponding seismic fragility curves can be obtained.

Each structure-motion sample with seismic acceleration peaks of 0.05 g, 0.075 g, 0.1 g, 0.2 g, 0.4 g, 0.6 g, and 0.8 g were considered. The seismic vulnerability analysis was performed, and the data for the SFIs of 6, 7, 8, and 9 are reported in Tab. 7. The corresponding seismic vulnerability curves are shown in Fig. 5-Fig. 8.

**Table 7:** Vulnerability data of single-story factory buildings with RC columns

Fortification intensity	PGA (g)	Probability of exceeding the limit state $P_f$			
		Minor damage	Medium damage	Severe damage	Collapse
6	0.05	0.10128	0.0039	0.000119	2.77E-08
	0.075	0.321553	0.032182	0.002096	1.9E-06
	0.1	0.54459	0.10128	0.011071	2.6E-05
	0.2	0.953948	0.617191	0.237143	0.006672
	0.4	0.999448	0.969706	0.805892	0.185101
	0.6	0.999986	0.997443	0.962962	0.510848
	0.8	0.999999	0.999725	0.992681	0.75247
7	0.05	0.070463	0.002127	5.39E-05	8.95E-09
	0.075	0.291482	0.026473	0.001594	1.25E-06
	0.1	0.54222	0.100226	0.010898	2.53E-05
	0.2	0.932972	0.54459	0.183627	0.0039
	0.4	0.99804	0.932972	0.686042	0.10128
	0.6	0.99989	0.989535	0.902442	0.321553
	0.8	0.99999	0.99804	0.969325	0.54459
8	0.05	0.003184	1.94E-05	1.46E-07	2.85E-12
	0.075	0.029198	0.000521	8.83E-06	7.17E-10
	0.1	0.099481	0.003783	0.000115	2.61E-08
	0.2	0.571781	0.114027	0.013243	3.48E-05
	0.4	0.950152	0.602583	0.225546	0.005993
	0.6	0.993852	0.868058	0.541265	0.048929
	0.8	0.99907	0.957778	0.761714	0.147521
9	0.05	0.00298	1.77E-05	1.30E-07	2.44E-12
	0.075	0.027735	0.000481	7.98E-06	6.24E-10
	0.1	0.090392	0.003219	9.26E-05	1.93E-08
	0.2	0.520536	0.090972	0.009426	2E-05
	0.4	0.925256	0.52195	0.168883	0.003288
	0.6	0.987913	0.807318	0.442126	0.02842
	0.8	0.997681	0.925756	0.666859	0.092139

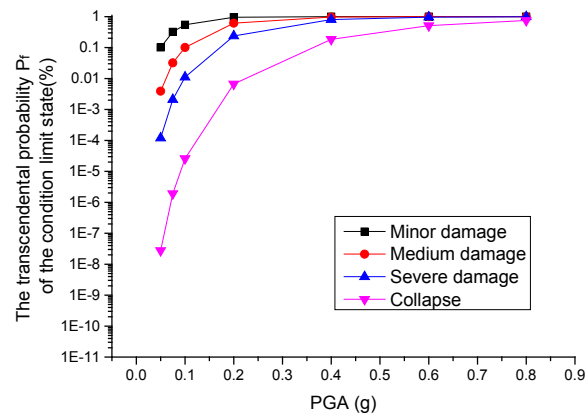


Figure 5: Seismic vulnerability curves of factory buildings for SFI of 6

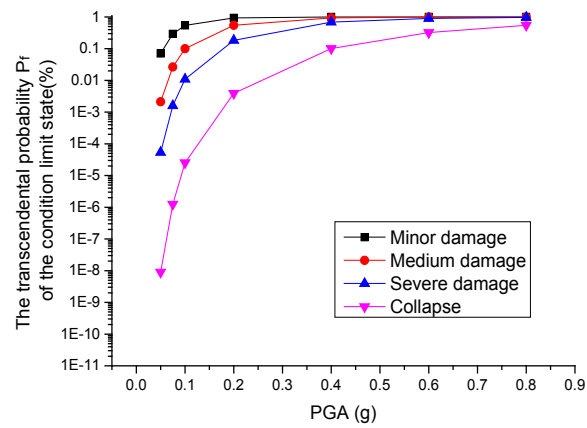
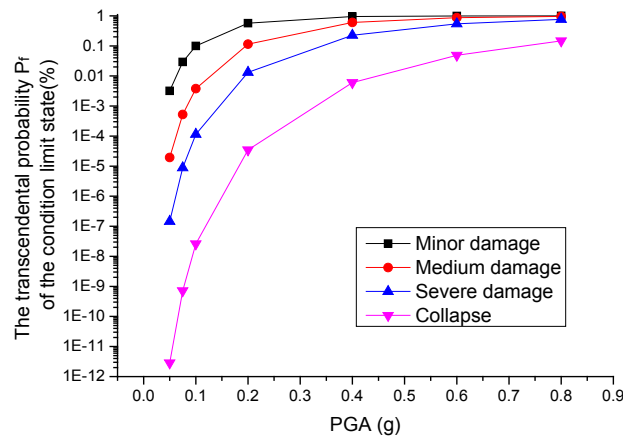
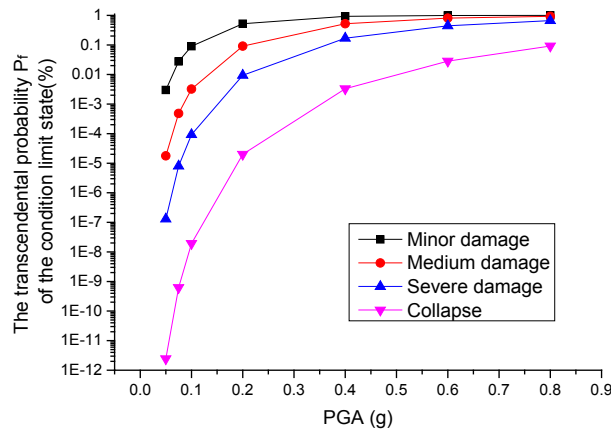


Figure 6: Seismic vulnerability curves of factory buildings for SFI of 7



**Figure 7:** Seismic vulnerability curves of factory buildings for SFI of 8



**Figure 8:** Seismic vulnerability curves of factory buildings for SFI of 9

From the vulnerability curves, it can be seen that under the same strength level of ground motions, the probability of exceeding the limit state of minor damage is highest. The probability of exceeding the limit state decreases from as the limit state progresses from minor damage to collapse. The probability exceeding the limit state of each failure class decreases with the improvement of the fortification level.

To analyze the seismic capacity of the factory structures more clearly, the probability of exceeding the limit states in Tab. 7 was transformed into a structural damage probability matrix. Taking the factory building with SFI of 6 subjected to the earthquake with PGA 0.05g as an example: the probability of exceeding the no damage state was  $100\% - 10.128\% = 89.87\%$ ; for the minor damage state the probability was  $10.128\% - 0.39\% = 9.74\%$ ; for the medium damage state it was  $0.39\% - 0.0119\% = 0.38\%$ ; for the severe damage state it

was  $0.0119\% - 0.00000227\% = 0.01\%$ ; and for the collapsed state the probability was  $2.77E-08\% = 0.00\%$ . In the same way, the probabilities of each failure state for factory buildings with different SFIs subjected to ground motions were calculated. These probability matrices of the structure damage for different SFIs are shown in Tab. 8-Tab. 11. In these tables, the relationship between the intensity and the peak of ground motion acceleration is given according to the (GB50011-2010) code for seismic design of buildings.

**Table 8:** Seismic damage probability matrix of factory buildings for SFI 6

Intensity	No damage	Minor damage	Medium damage	Severe damage	Collapse
Intensity 6 (0.05 g)	89.87	9.74	0.38	0.01	0.00
Intensity 7 (0.10 g)	45.54	44.33	9.02	1.11	0.00
Intensity 8 (0.20 g)	4.60	33.68	38.00	23.05	0.67
Intensity 9 (0.40 g)	0.06	2.97	16.38	62.08	18.51
Intensity 10 (0.80 g)	0.00	0.03	0.70	24.02	75.25

**Table 9:** Seismic damage probability matrix of factory buildings for SFI of 7

Intensity	No damage	Minor damage	Medium damage	Severe damage	Collapse
Intensity 6 (0.05 g)	92.95	6.83	0.21	0.01	0.00
Intensity 7 (0.10 g)	45.78	44.20	8.93	1.09	0.00
Intensity 8 (0.20 g)	6.70	38.84	36.10	17.97	0.39
Intensity 9 (0.40 g)	0.19	6.51	24.69	58.48	10.13
Intensity 10 (0.80 g)	0.00	0.19	2.87	42.47	54.46

**Table 10:** Seismic damage probability matrix of factory buildings for SFI of 8

Intensity	No damage	Minor damage	Medium damage	Severe damage	Collapse
Intensity 6 (0.05 g)	99.68	0.32	0.00	0.00	0.00
Intensity 7 (0.10 g)	90.05	9.57	0.37	0.01	0.00
Intensity 8 (0.20 g)	42.82	45.78	10.08	1.32	0.00
Intensity 9 (0.40 g)	4.98	34.76	37.70	21.96	0.06
Intensity 10 (0.80 g)	0.09	4.13	19.61	61.42	14.75

**Table 11:** Seismic damage probability matrix of factory buildings for SFI of 9

Intensity	No damage	Minor damage	Medium damage	Severe damage	Collapse
Intensity 6 (0.05 g)	99.70	0.30	0.00	0.00	0.00
Intensity 7 (0.10 g)	90.96	8.72	0.31	0.01	0.00
Intensity 8 (0.20 g)	47.95	42.96	8.15	0.94	0.00
Intensity 9 (0.40 g)	7.47	40.33	35.31	16.56	0.33
Intensity 10 (0.80 g)	0.23	7.19	25.89	57.47	9.22

The probability matrices in Tab. 6-Tab. 9 allow the seismic performance of the factory building with different SFIs to be evaluated with respect to the seismic fortification level.

From Tab. 6, it can be seen that when the factory building designed with a SFI of 6 was subjected to a local intensity earthquake influence 0.05 g, the probability of no damage and minor damage was cumulatively 99.61%, indicating that the objective of “no damage in moderate earthquakes” can be achieved. Thus, it can be shown that the seismic fortification objective of “no damage in minor earthquakes, mendable in moderate earthquakes” of the factory building with as SFI of 6 can be achieved. When the factory building subjected to strong earthquake whose PGA was 0.2 g, the probability of no damage, minor damage, and medium damage was 76.28% while the probability of severe damage was 23.05%, and that

of collapse was 0.67%. Thus, it can be shown that the seismic fortification objective of “no collapsing in strong earthquakes” for a factory building with SFI of 6 can be achieved. Furthermore, even the objective of “mendable in strong earthquakes” can be achieved.

From Tab. 7, it can be seen that when the factory building designed with a SFI of 7 was subjected to the earthquake whose PGA was 0.05 g, the cumulative probability of no damage and minor damage was 99.78%, and the objective of “no damage in moderate earthquakes” is realized. When the factory building was subjected to the local fortification intensity earthquake with PGA of 0.01 g, the probability of no damage, minor damage, and medium damage was a cumulative 98.91%. The probability of severe damage was 1.09%, and there was zero probability of collapse, indicating that the objective of “mendable in moderate earthquakes” was achieved. When the factory building was subjected to an earthquake of 0.4 g, the probability of minor damage, medium damage, and severe damage was 89.68%. The probability of collapse was 10.13%. Thus, it can be shown that the seismic fortification objective of “no collapsing in strong earthquakes” of the factory building with seismic fortification 7 was realized.

From Tab. 8, it can be seen that when the factory building designed in SFI 8 was subjected to a 0.10 g earthquake, the sum of the probabilities of no damage and minor damage was 99.62%. Thus, the objective of “no damage in moderate earthquakes” was reached. When the factory building was subjected to an earthquake intensity of 0.20 g, the combined probability of no damage, minor damage and medium damage was 98.68%. The probability of severe damage was 1.32%, and there was zero collapse probability. This means that objective of “mendable in moderate earthquakes” can be achieved. When the factory building was subjected to earthquake 0.4 g, the probability of collapse was 0.60%. Thus, the objective of “no collapsing in strong earthquakes” can be realized. When the factory building was subjected to the super rare earthquake of 0.8 g, the probability of minor damage, medium damage, and severe damage was a cumulative 85.16%. The probability of collapse was 14.75%. Thus, “no collapsing in super strong earthquakes” for factory buildings with seismic fortification 8 is reasonably achieved.

From Tab. 9, it can be seen that when the factory building designed in SFI 9 is subjected to a 0.10g earthquake, the probability of no damage and minor damage was 99.68%. For a 0.20g earthquake, the no damage and minor damage probability was 90.91%. No collapsing probability is seen for either of these earthquake levels. Consequently, the seismic fortification objective of “no collapsing in strong earthquakes” of the factory building with seismic fortification 9 can be reached. When the factory building is subjected to the local fortification intensity earthquake 0.40 g, the probability of no damage, minor damage, and medium damage was 83.11%. The probability of severe damage and collapse were 16.56% and 0.33%, indicating that the objective of “mendable in moderate earthquakes” was reasonably achieved. When the factory building was subjected to an earthquake of 0.8 g, the probability of minor damage, medium damage, and severe was 90.78%. The probability of collapse was 9.22%. Thus, it can be shown that the seismic fortification objective of “no collapsing in strong earthquakes” of the factory building with seismic fortification 9 can be reasonably achieved.

To summarize, it was seen that the factory buildings designed with the SFI of 6 met the seismic objective of “no damage in moderate earthquakes, mendable in strong earthquakes”.

The factory buildings designed with the SFIs of 7 and 8 realized the seismic objective of “no collapse in strong earthquakes” but also that of “no collapse in super strong earthquakes”. However, the damage probability of the factory buildings with SFI 8 was slightly more than that with SFI 7. For the factory buildings designed with an SFI of 9, the seismic objective of “mendable in moderate earthquakes” was reasonably achieved. Therefore, compared to the factory buildings designed with higher SFI, the factory buildings designed with lower SFI had a better performance at reaching their seismic objectives.

## **6 Conclusion**

In this paper, the seismic vulnerability of single-story factory buildings with RC columns and a light roof was studied through nonlinear time history analysis and finite element analysis. In the seismic vulnerability analysis, the combination of the Latin hypercube sampling technique and the orthogonal design was used. Given a sufficient sampling rate, the sampling number was reduced, and the efficiency and accuracy of the numerical simulation of seismic vulnerability were improved. The seismic vulnerability curves and damage matrix of buildings under seismic fortification were given. The results showed that the seismic performance of different factory buildings under different horizontal ground motions could be evaluated accurately. It can also be used for seismic damage prediction and analysis of cities or enterprises, as well as for the quick and accurate assessment of seismic damage loss after the earthquake. At the same time, it also helps government departments to formulate reasonable policies for mitigating earthquake disaster, conducting emergency rescues, and post-earthquake reconstruction.

From the analysis of the seismic vulnerability curves and failure matrices, it was shown that:

- (1) For the SFI 6, the seismic fortification objective of “no damage in minor earthquakes, mendable in moderate earthquakes, no collapsing in strong earthquakes” was well satisfied. Additionally, the objective of “no damage in moderate earthquakes, mendable in strong earthquakes” was met.
- (2) For the SFIs of 7 and 8, the objective of “no damage in minor earthquakes, mendable in moderate earthquakes, no collapsing in strong earthquakes” was reached as well as “no collapse in super strong earthquakes”.
- (3) With an SFI of 9, “no damage in minor earthquakes, no collapsing in strong earthquakes” was realized and the objective of “mendable in moderate earthquakes” was reasonably satisfied.
- (4) Compared with the factory buildings designed in high fortification intensities, the low fortification designs performed better at meeting fortification objectives.
- (5) The seismic vulnerability of the single-story factory buildings with RC columns and a light roof for seismic fortification was analyzed here; however, it was shown from previous seismic damage analysis that the damage of factory buildings with heavy roofs are more serious than those with light roofs. Therefore, it is necessary to further analyze and study the seismic vulnerability of the factory buildings with heavy roofs in the future.

**Acknowledgment:** The research is supported by the Basic research fund from the Institute of Engineering Mechanics China Earthquake Administration (Grant No.

2014A01), the Plan of Heilongjiang province application technology research and development (Grant No. GX16C007), and the Program for Innovative Research Team in China Earthquake Administration.

## References

**Banon, H.; Biggs, J.; Irvine, H.** (1981): Seismic damage in reinforced concrete frames. *Journal of the Structural Division*, vol. 107, no. 9, pp. 1713-1729.

**Chen, S.; Liu, T.; Li, G.; Liu, Q.; Sun, J.** (2017): Optimal design and dynamic impact tests of removable bollards. *Earthquake Engineering & Engineering Vibration*, vol. 16, pp. 793-802.

**Earthquake Relief in Wenchuan Great Earthquake (Book 4: Earthquake Disaster).** (2015). China.

**Felipe, A. C.; Gerhard, V.; Vladimir, B.** (2010): An algorithm for fast optimal Latin hypercube design of experiments. *Numerical Method in Engineering*, vol. 82, pp. 135-156.

**Fuchs S.; Keiler M.; Glade T.** (2017): Editorial to the special issue on resilience and vulnerability assessments in natural hazard and risk analysis. *Nature Hazards and Earth System Science*, vol. 17, pp. 1203-1206.

**GB50011-2001** (2008 Edition): *Code for Seismic Design of Buildings*. China.

**GB50011-2001** (2001): *Code for Seismic Design of Buildings*. China.

**GB50011-2010** (2010): *Code for Seismic Design of Buildings*. China.

**GBJ-89** (1989). *Code for Seismic Design of Buildings*. China.

**Hamed, A.; Nuno, M.; Paulo, B. L.; Neda, H. S.** (2016): Empirical seismic vulnerability analysis for masonry buildings based on school buildings survey in Iran. *Bull Earthquake Engineering*, vol. 14, pp. 3195-3229.

**Howard, H.; Hwang, M.; Jaw, J.** (1990): Probabilistic damage analysis of structures. *Structural Engineering*, vol. 116, pp. 1992-2007.

**Li, L.** (2010): *The Seismic Damage and Seismic Response Analysis on Single-Story Factory Buildings with Reinforced Concrete Columns (Ph.D. Thesis)*. Institute of Engineering Mechanics, China.

**Lam, H. F.; Hu, J.; Yang, J. H.** (2017): Bayesian operational modal analysis and Markov chain Monte Carlo-based model updating of a factory building. *Engineering Structures*, vol. 132, pp. 314-336.

**Lee, V. W.; Manić, M. I.; Bulajić, B. Đ.; Herak, D.; Herak, M. et al.** (2015): Microzonation of Banja Luka for performance-based earthquake-resistant design. *Soil Dynamics and Earthquake Engineering*, vol. 78, pp. 71-88.

**Li, Q.** (2011): *Study and Application of Incremental Dynamic Analysis Method (Ph.D. Thesis)*. Xi'an University of Architecture and Technology, China.

**Lü, D.; Yu, X.; Pan, F.; Wang, G.** (2010): Probabilistic seismic demand analysis of structures based on an improved cloud method. *World Earthquake Engineering*, vol. 26, no. 1, pp. 8-15.

- Matjaz, D.** (2009): Incremental dynamic analysis with consideration of modeling uncertainties. *Earthquake Engineering Structure Dynamics*, vol. 38, pp. 805-825.
- Mauro, N.; Gustavo, A.; Saúl, L.** (2018): Uniform fragility spectra for the performance-based seismic design of structures considering variabilities in structural properties. *Earthquake Engineering Structure Dynamics*, vol. 47, pp. 1742-1754.
- Mirko, K.; Peter, F.; Matjaž, D.** (2014): Approximate seismic risk assessment of building structures with explicit consideration of uncertainties. *Earthquake Engineering Structure Dynamics*, vol. 43, pp. 1483-1502.
- Ricardo, M.** (2016): Sampling based numerical seismic assessment of continuous span RC bridges. *Engineering Structures*, vol. 118, pp. 407-420.
- Roy, C. S.; Roy, D.; Vasu, R. M.** (2013): Variance-reduced particle filters for structural system identification problems. *Engineering Mechanics*, vol. 139, pp. 210-218.
- Seymour, M. J.; Ahsan, K.** (2014): Performance-based design and optimization of uncertain wind-excited dynamic building systems. *Engineering Structures*, vol. 78, pp. 133-144.
- Wu, Z.; Wang, D.; Patrick, N. O.; Zhao, K.; Zhang, W.** (2017): Efficient space-filling and near-orthogonality sequential Latin hypercube for computer experiments. *Computer Methods in Applied Mechanics & Engineering*, vol. 324, pp. 348-365.
- Zhang, G. D.; Alberdi, R.; Khandelwal, K.** (2016): Analysis of three-dimensional curved beams using isogeometric approach. *Engineering Structures*, vol. 117, pp. 560-574.
- Zhu, T.; Heidebrecht, A.; Tso, W.** (1988): Effect of peak ground acceleration to velocity ratio on ductility demand of inelastic systems. *Earthquake Engineering Structural Dynamics*, vol. 16, pp. 63-79.